cells

MDPI

Article

Nutlin-3a-Mediated IL17RB Repression Leads to Enhanced p53 Responses via Modulating the Cellular Levels of p21 and Bcl-2

Alessandro Provvido, Can Sabancelebi, Shiva Shastri, Joseph Sachakov, Olivia Hu, Ivana Vancurova and Yan Zhu *

Department of Biological Sciences, St. John's University, Queens, NY 11439, USA
* Correspondence: zhuy1@stjohns.edu

Abstract

The interleukin 17 (IL17) cytokine family and its receptors are essential to normal host immune function, and their dysregulation has been linked to a broad range of human diseases, most notably inflammatory conditions and cancer. Interleukin 17 receptor B (IL17RB), in particular, has emerged as an important contributor to tumorigenesis. Here we identified IL17RB as a target of p53-mediated repression. Nutlin-3a treatment substantially decreased IL17RB expression across several cell lines harboring wild-type p53, but not in mutant-p53 or p53-null lines, and the effect was not reversed by proteasome inhibition. Depletion of either p53 or p21 partially rescued IL17RB expression. Functionally, IL17RB depletion enhanced, whereas IL17RB overexpression attenuated, nutlin-3a-induced inhibition of cell proliferation and migration. In line with this, IL17RB knockdown increased, while IL17RB overexpression reduced, nutlin-3a-induced p21 expression. IL17B treatment attenuated nutlin-3a-mediated p21 induction and Bcl-2 repression. Bioinformatic analysis showed that IL17RB expression was higher in prostate and colon tumors than in their respective matched normal tissue. Interestingly, IL17RB correlated modestly but significantly with Bcl-2 and inversely with p21 in colon tumors. Collectively, these findings indicate that p53-dependent repression of IL17RB reinforces p53 responses, revealing a functional connection between inflammatory signaling and p53-dependent tumor suppression.

Keywords: IL17RB; p53; nutlin-3a; p21; Bcl-2; IL17B; tumor suppression

1. Introduction

The p53 pathway is impaired in almost all human cancers, and about half of all tumors sustain mutations in the *TP53* gene [1–3]. In response to a variety of stress signals, the p53 tumor suppressor primarily functions as a sequence-specific transcription factor to induce (or, in some cases, repress) genes that regulate various cellular processes, including cell cycle arrest, apoptosis, metabolism, and innate immunity [4–9]. Besides curbing tumorigenesis by regulating cellular homeostasis, p53 has also been shown to play a role in inflammatory responses [10–12]. p53 dysfunction in tumors can enhance chronic inflammation and then promote tumor progression [6,10].

The IL17 cytokine family (IL17A to IL17F) and receptors (IL17R; IL17RA to IL17RE) play crucial roles in host immune responses. Their dysregulation has been associated with many human diseases, notably inflammation and cancer [13–15]. Several studies

Academic Editor: Amancio Carnero

Received: 30 September 2026
Revised: 7 November 2026
Accepted: 9 November 2026
Published: 12 November 2026

Copyright: © 2026 by the authors. Licensee MDPI, Basel, Switzerland. This article is an open access article distributed under the terms and conditions of the Creative Commons Attribution (CC BY) license.

highlighted the role of the IL17B/IL17RB pathway in cancer [16–23]. It has been shown that IL17RB is overexpressed in various cancers, activating multiple signaling pathways that promote tumorigenesis [24,25]. Targeting IL17B/IL17RB signaling with an anti-IL17RB antibody has been reported to block metastasis and tumor growth in xenograft models for breast and pancreatic cancers [26–28].

When we reanalyzed the global gene expression analysis from a previous study [29], IL17RB was identified as a gene strongly repressed by MDM2/MDMX inhibitors. Here, we focus on the functional connection between p53 and IL17RB. We characterized nutlin-3a (a well-studied inhibitor of the p53 pathway)-mediated repression of IL17RB in various cell lines and examined its role in p53-mediated tumor suppression. Our data demonstrated that p53 is required for nutlin-3a-mediated repression of IL17RB expression. p53-mediated repression of IL17RB likely occurs indirectly, as no p53 binding was detected on the IL17RB promoter region in ChIP assays. Depletion of p53 or p21 (a major mediator of p53-dependent repression) rescued IL17RB levels in nutlin-3a-treated cells. We showed that IL17RB depletion enhanced nutlin-3a-induced inhibition of cell proliferation, whereas IL17RB overexpression attenuated nutlin-3a-induced inhibition of cell growth and migration. In correlation, IL17RB knockdown enhances, while IL17RB overexpression reduces nutlin-3a-induced p21 expression. IL17B treatment diminishes the effect of nutlin-3a on Bcl-2 repression and p21 induction. Furthermore, bioinformatic analysis revealed that IL17RB is overexpressed in prostate and colon cancer samples in comparison to normal samples. A moderate but significant positive correlation between IL17RB and Bcl-2 and a negative correlation between IL17RB and p21 were observed in colon tumors. Our results supported the literature on IL17RB signaling as oncogenic and suggested that its repression may contribute to p53's tumor-suppressive function by modulating cellular levels of p21 and Bcl-2.

2. Materials and Methods

2.1. Cell Culture and Plasmids

LNCaP cells (CRL-1740; ATCC, Rockville, MD, USA) were grown in RPMI medium containing 10% fetal bovine serum (FBS) at 37 °C. 22Rv1, DU145, PC3, HCT116 p53 +/+, HCT116 p53 −/−, HCT116 p21 −/− (a kind gift from Dr. Carol Prives, Columbia University), and U2OS cells (HTB-96; ATCC, Rockville, MD, USA) were grown in Dulbecco modified Eagle medium containing 10% FBS at 37 °C. pcDNA3-IL17RB was constructed by subcloning IL17RB fragment from pDNR-IL17RB construct (HsCD0002711; DNASU repository) into pcDNA3 vector, and verified by DNA sequencing.

2.2. Antibodies and Reagents

Commercially obtained antibodies were used to detect the following proteins or epitopes: IL17RB (rabbit polyclonal antibody; NBP2-43767, Novus Biologicals, Centennial, CO, USA; 1:3000 dilution), Actin (mouse monoclonal antibody; Genscript, Piscataway, NJ, USA; 1:10,000 dilution), MDM2 (rabbit monoclonal antibody; D1V2Z, Cell signaling, Danvers, MA, USA; 1:2000 dilution), p21 (rabbit monoclonal antibody; 12D1, Cell signaling; 1:4000 dilution), Bcl-2 (mouse monoclonal antibody; c-2, Santa Cruz Biotechnology, Dallas, TX, USA; 1:250 dilution), p53 (mouse monoclonal antibody; DO-1, Santa Cruz Biotechnology; 1:500 dilution). Chemical reagents used in this study were as follows: nutlin-3 (10 μM; Sigma-Aldrich, St. Louis, MO, USA), Doxorubicin (1 μM; Sigma-Aldrich), Etoposide (15 μM; Sigma-Aldrich), Actinomycin D (5 nM; Sigma-Aldrich), MG132 (20 μM; Calbiochem, San Diego, CA, USA), and ALLN (10 μM; Sigma-Aldrich). Recombinant Human IL-17B (50 ng/mL) (CHO) Protein was purchased from the R&D System (Minneapolis, MN, USA).

2.3. DNA Transfection and siRNA Transfection

Cell DNA transfections were performed using Lipofectamine 3000 (Thermo Fisher Scientific, Waltham, MA, USA) following the manufacturer's protocol. In all transfection experiments, pcDNA3 plasmid was added to ensure equal amounts of total DNA were transfected. Cell siRNA transfections were carried out using DharmaFECT 1 (Dharmacon, Horizon Discovery, Lafayette, CO, USA) with 50 nM of control siRNA (Allstar negative control siRNA; Qiagen, Germantown, MD, USA) or siRNA targeting p53 (605 and 606; Sigma-Aldrich), IL17RB (sc-39964; Santa Cruz Biotechnology and siGENOME human IL17RB siRNA-SMARTpool; Dharmacon), or p21. The target sequences for p21 are: p21siRNA #1 5′-CAGTTTGTGTGTCTTAATTAT-3′; p21 siRNA #2 5′-CTGGCATT-AGAATTATTTAAA-3′ [30].

2.4. Western Blot Analysis

Cells were lysed in Lysis buffer containing 10 mM Tris (pH 7.5), 1 mM EDTA, 150 mM NaCl, 10% glycerol, 0.5% NP-40, 5 mM NaF, 0.5 mM sodium orthovanadate, 1 mM dithiothreitol, 0.1 mM phenylmethylsulfonyl fluoride, and protease inhibitors (Sigma). Protein concentrations were determined by a Bio-Rad protein assay. Equal amounts of total protein were separated by SDS-polyacrylamide gel electrophoresis and transferred to nitrocellulose membranes (Cytiva, Marlborough, MA, USA). After blocking with 1% non-fat dry milk in 1× PBS containing 0.1% Tween-20 (blocking buffer) for 1 h at room temperature, the membrane was incubated with the indicated primary antibodies diluted in blocking buffer at 4 °C overnight or at room temperature for 2 h, followed by incubation with HRP-conjugated secondary antibodies for 1 h at room temperature. Proteins were visualized using ECL reagents and a chemiluminescence imaging system (Kindle Bioscience, Greenwich, CT, USA). Densitometric quantification of the immunoblots was performed using ImageJ software (version 1.53, NIH, Bethesda, MD, USA). For each sample, the background-subtracted integrated density of the target protein band was normalized to the corresponding Actin band. Data are expressed as fold changes relative to the control group.

2.5. Luciferase Reporter Assay

The *IL17RB* promoter DNA fragment (1.5 kb upstream of the transcription start site) was amplified by polymerase chain reaction with Phusion High-Fidelity DNA Polymerases (Thermofisher Scientific) and inserted into a p5xATF6-GL3 plasmid (Addgene, Plasmid #11976) multiple cloning site with *Hind*III/*Xho*I to replace the original 5XATF6 insertion. Primers used are: Forward: 5′-CAAaagcttCCAGTCCCAGGCAGG-3′ and Reverse: 5′-CAAActcgagACTGCGCGGGATCCA-3′. The cloned IL17RB-luc plasmid was verified by DNA sequencing. For the dual-luciferase reporter assay, LNCaP cells were plated in 96-well plates and transfected with 5 ng of pRL vector (Promega, Madison, WI, USA), with or without 20 ng of IL17RB-luc, in triplicate. Twenty-four hours after transfection, cells transfected with IL17RB-luc were treated with DMSO or nutlin-3a (10 μM) for 24 h, and luciferase activity was assessed using the dual-glo luciferase reporter assay system (Promega). The firefly-to-Renilla luminescence ratio for each well was calculated. Relative luciferase activity was normalized to the ratio from the pRL vector alone samples.

2.6. Chromatin Immunoprecipitation Assay

Chromatin Immunoprecipitation (ChIP) experiments were carried out as previously described [31]. Cells were crosslinked with 1% formaldehyde in PBS for 15 min at room temperature. A final concentration of 125 mM glycine was added for 5 min at room temperature to stop crosslinking. After washing twice with cold PBS, cells were lysed by incubating on ice for 20 min in RIPA buffer (50 mM Tris-HCl, pH 8.0, 150 mM NaCl, 1% NP-40, 0.5% deoxycholate, 0.1% SDS, 5 mM EDTA, and protease inhibitors) and then sonicated with a Qsonica 125 for a total of 4 min (8 pulses of 30 s on, 30 s off) in an ice-water bath at 50% amplitude, followed by centrifugation at 10,000 rpm for 10 min. The supernatant was precleared for 1 h with protein A/G beads (preblocked with 1 mg/mL BSA and 0.3 mg/mL salmon sperm DNA). The pre-cleared supernatant was incubated with anti-p53 (DO-1) antibody or normal mouse IgG together with pre-blocked protein A/G beads overnight at 4 °C. The beads were recovered and washed twice with RIPA buffer, four times with ChIP Wash Buffer (100 mM Tris-HCl, pH 8.5, 500 mM LiCl, 1% NP-40, 1% deoxycholate), once with RIPA buffer, and twice with TE buffer (10 mM Tris-HCl, pH 8.0 and 1 mM EDTA). The antibody/protein/DNA complexes were eluted at 65 °C for 15 min with 1% SDS and incubated with proteinase K (Thermo Fisher Scientific) at 65 °C overnight to reverse crosslinking. DNA was purified using QIAquick PCR purification kit (Qiagen). The ChIP-qPCR assay was performed using Power SYBR Green Master Mix (Thermo Fisher Scientific) with the Bio-Rad CFX96 system (Bio-Rad, Hercules, CA, USA). The primer sequences are: p21 5′ RE (Forward: 5′-AGCAGGCTGTGGCTCTGATT-3′; Reverse: 5′-CAAAATAGCCACCAGCCTCTTCT-3′); p21 neg (+11443 region) (Forward: 5′-TCTGTCTCGGCAGCTGACAT -3′; Reverse: 5′-ACCACAAAAGATCAAGGTGAGTGA-3′); Chromosome 4, Gene Desert (hg38) (Forward: 5′-AGCCACCTGTAATCCCAACA-3′; Reverse: 5′-TGCTGTTTGTGTCTGTGTGT-3′); IL17RB primer set 1 (Core/TSS) (Forward: 5′-GGGCCCGCCCTCTGTTCG-3′; Reverse: 5′-CCAGGCCACCCGCACGCT-3′); IL17RB primer set 2 (−240) (Forward: 5′-CAGCTGGCTCACTGCATG-3′; Reverse: 5′-GGGAGGGATGGGCCGTGT-3′); IL17RB primer set 3 (−528) (Forward: 5′-AGCCCCTCCGGGCTAGCG-3′; Reverse: 5′-CCCGAGTCGCCCCGGGTGA-3′); IL17RB primer set 4 (−272) (Forward: 5′-CAGCTGGCTCCAGCGGAGG-3′; Reverse: 5′-CAGCCAGGTGCATCAGCTGC-3′).

2.7. Cell Proliferation Assay

Cell proliferation was measured using the CellTiter 96® Aqueous One Solution Cell Proliferation Assay (MTS, Promega) following the manufacturer's protocol. LNCaP cells were transfected with control siRNA or siRNA targeting IL17RB, and trypsinized 24 h after transfection. Approximately 3000 cells per well were plated in 96-well plates in 150 µL of complete RPMI medium. Twenty hours later, triplicate cell cultures were treated with DMSO or nutlin-3a (10 µM) for 24 h and imaged under a light microscope (Nikon Ts2, Tokyo, Japan). The medium was then removed and replaced with 100 µL of fresh complete medium and 10 µL of CellTiter 96® Aqueous One Solution, and the cells were incubated for 2–4 h at 37 °C. Absorbance at O.D.490 nm was read on a Tecan Spark Microplate Reader. The results are expressed as means±s.d. and graphed using GraphPad Prism version 10.2.0 for Windows (GraphPad Software, Boston, MA, USA).

2.8. Colony Formation Assay

A total of 1×10^4 HCT116 cells, with or without IL17RB overexpression, were plated in a 24-well plate and then treated with DMSO or nutlin-3a (10 µM) as indicated. The medium was replaced every other day. Fourteen days after treatment, the cells were fixed and stained with crystal violet (0.05% in 20% ethanol) to visualize cell viability.

2.9. Transwell Migration Assay

A total of 3 × 10^4 U2OS cells (transfected with pcDNA3 or cmv-IL17RB) in 100 μL serum-free DMEM (with or without 10 μM nutlin-3a) were seeded in the upper chamber of the 24-well Transwell insert (8 μm pore size; Corning Inc., Corning, NY, USA,). Then, 700 μL of DMEM with 2% FBS was added to the lower chamber. Sixteen (without nutlin-3a treatment) or twenty-one (with nutlin-3a treatment) hours later, non-migrated cells from the apical side of the Transwell insert membrane were removed using a cotton-tipped applicator. Migrated cells were fixed with 4% Paraformaldehyde in PBS, stained with crystal violet (0.05% in 20% ethanol), and visualized with an inverted microscope.

2.10. RNA Extraction and Quantitative RT-PCR Analysis

LNCaP or HCT116 cells were plated in 6-well plates and transfected with the indicated siRNAs targeting p53, p21, or IL17RB. Twenty-four hours after transfection, cells were treated with DMSO, nutlin-3a (10 μM), or Doxorubicin (1 μM) as indicated, and harvested 24 h after treatment. RNA was extracted using a Qiagen RNeasy mini-kit, and cDNA was synthesized with the QuantiTect reverse transcription kit (Qiagen). Quantitative real-time PCR was carried out using Power SYBR Green Master Mix (Thermo Fisher Scientific) on a Bio-Rad CFX 96. Relative mRNA levels were calculated by the comparative Ct method (ΔΔCT method) and normalized to RPL32. The results are expressed as means±s.d., graphed, and statistically analyzed using an unpaired t-test with GraphPad Prism. Primer sequences are: p21 (F: 5′- GGCGGCAGACCAGCATGACAGATT-3′; R: 5′-GCAGGGGGCGGCCAGGGTAT-3′), IL17RB (F: 5′-AGGGACCTCCGAGTAGAACC-3′; R: 5′-CTTGGTGGCCTTCAACAAGC-3′), IL17RA (F: 5′-CTGATGGGGACCCAAACCAC-3′; R: 5′-CCACAGGGTGAAGCTCACAC-3′), and L32 (F: 5′-TTCCTGGTCCACAATGTCAAG-3′; R: 5′-TGTGAGCGATCTCAGCAC-3′).

2.11. Gene Expression Analysis

IL17RB mRNA expression levels in normal prostate gland and prostate carcinoma samples were obtained from www.oncomine.com using the Lapointe Prostate (GSE3933 [32]) and Taylor Prostate (GSE21034 [33]) datasets. Statistical significance for two-class comparisons (cancer vs. normal) was assessed using Student's *t*-test. In addition, levels of IL17RB mRNA in paired normal or cancer samples were retrieved from tnmplot.com [34]. This platform integrates data from four primary sources: Gene Chip data manually curated from NCBI-GEO, RNA-seq data from TCGA (The Cancer Genome Atlas), GTEx (Genotype-Tissue Expression), and TARGET (Therapeutically Applicable Research to Generate Effective Treatments). Gene Chip data were normalized using the MAS5 algorithm, with probe-to-gene mapping performed using JetSet annotation. RNA-seq raw counts from TCGA, TARGET, and GTEx were normalized using the DESeq2 package. Statistical significance for RNA-seq comparisons between tumor and normal tissues (prostate adenocarcinoma and colon adenocarcinoma) was determined using the Mann–Whitney test. Stage analysis of IL17RB levels in prostate and colon tissues was also retrieved from tnmplot.com. Statistical significance was determined using the Kruskal–Wallis test. Spearman correlation analysis was performed using Gene Chip data from colon tumor samples, and RNA-seq data from prostate tumor samples. The significance of the correlation coefficients was evaluated using a t-test based on the correlation coefficient and sample size.

3. Results

3.1. Nutline-3a Treatment Downregulates IL17RB

To explore the role of p53 in inflammation regulation, we reanalyzed the global gene expression profile from a previous study [29] and identified IL17RB as one of the most

repressed cytokine/chemokine receptor genes in LNCaP cells co-treated with nutlin-3a [35] (an MDM2 inhibitor) and NSC207895 [36] (NSC; an MDMX inhibitor), as well as in LNCaP cells treated with nutlin-3a alone. Using quantitative RT-PCR, we confirmed that nutlin-3a downregulates IL17RB at the mRNA level. As shown in Figure 1A, the mRNA levels of IL17RB but not IL17RA, another member of the IL17 receptor family, were dramatically reduced in LNCaP cells treated with nutlin-3a. Using Western blot analysis, we observed that nutlin-3a reduced IL17RB levels in LNCaP cells in a dose-dependent manner (Figure 1B). Nutlin-3a-mediated repression of IL17RB was also observed in 22RV1 cells (Figure 1C), a prostate cancer cell line containing one wild-type p53 allele, but not in DU145, a prostate cancer cell line with mutant p53, or PC3, a p53-null prostate cancer cell line (Figure 1D). Note that in addition to the full-length protein, a prominent, faster-migrating IL17RB species (between 37 and 50 kDa) was detected by Western blot in 22RV1 cells, and its intensity also decreased upon nutlin-3a treatment. To extend our observation to other non-prostate cell lines, we treated U2OS, a wild-type p53-containing osteosarcoma cell line, and HCT116 isogenic cell lines (p53 +/+ and p53 −/−) with nutlin-3a and examined IL17RB levels by Western blot and/or quantitative RT-PCR analysis. We found that nutlin-3a treatment reduced IL17RB at both the mRNA and protein levels in U2OS (Figure 1E,F), and HCT116 (Figure 1G,H), but not in HCT116 p53 −/− cells (Figure 1H). A prominent, faster-migrating IL17RB species was detected by Western blot in HCT116 cells, but its intensity remained unchanged upon nutlin-3a treatment, unlike in 22RV1 cells. Together, these data indicated a nutlin-3a/wild-type p53-dependent mechanism for repressing IL17RB expression. Our subsequent experiments have focused on the full-length form of IL17RB in LNCaP and HCT116 cells.

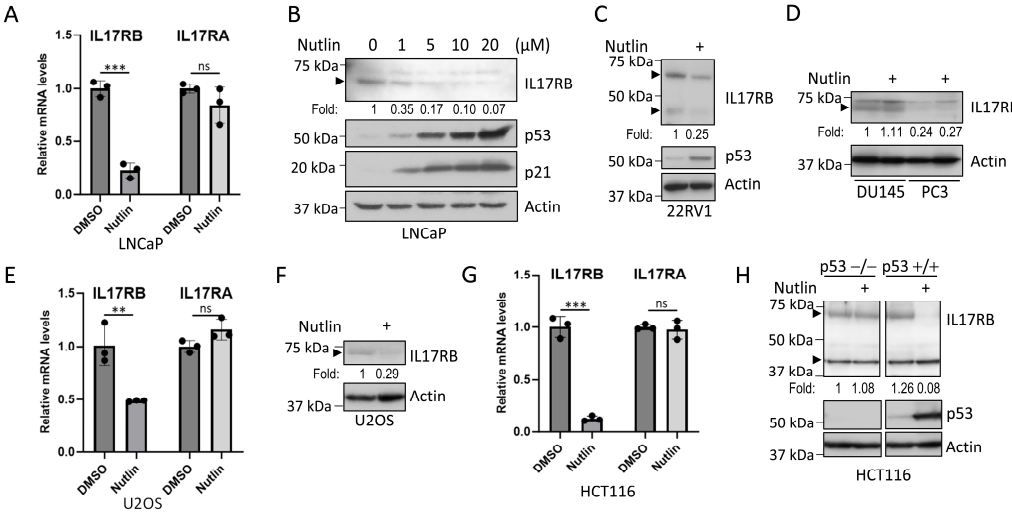


Figure 1. Nutlin-3a treatment downregulates IL17RB. (**A**) Relative mRNA levels of IL17RB and IL17RA were measured by qRT-PCR in LNCaP cells treated with DMSO or nutlin-3a (10 μM) for 24 h (n = 3; *** $p < 0.001$). (**B**) Western blot analysis of LNCaP cells treated with DMSO or increasing concentrations of nutlin-3a (1, 5, 10, or 20 μM) for 24 h. The arrow indicates full-length IL17RB. (**C**) Western blot analysis of 22RV1 cells treated with DMSO or nutlin-3a (10 μM) for 24 h. Top arrow: full-length IL17RB. Bottom arrow: faster-migrating species of IL17RB. (**D**) Western blot analysis of DU145 and PC3 cells treated with DMSO or nutlin-3a (10 μM) for 24 h. The arrow indicates full-length IL17RB. (**E**) Relative mRNA levels of IL17RB and IL17RA were measured by qRT-PCR in U2OS cells treated with DMSO or nutlin-3a (10 μM) for 24 h (n = 3; ** $p < 0.01$). (**F**) Western blot analysis of U2OS cells treated with DMSO or nutlin-3a (10 μM) for 24 h. The arrow indicates full-length IL17RB. (**G**) Relative mRNA levels of IL17RB and IL17RA were measured by qRT-PCR in HCT116 cells treated with DMSO or nutlin-3a (10 μM) for 24 h (n = 3; *** $p < 0.001$). (**H**) Western blot

analysis of HCT116 (p53 −/− and p53 +/+) cells treated with DMSO, nutlin-3a (10 μM), or Dox (doxorubicin; 1 μM) for 24 h. Top arrow: Full-length IL17RB. Bottom arrow: Faster-migrating species of IL17RB. Quantification of the IL17RB immunoblots was performed using ImageJ software. Fold: Relative full-length IL17RB amount.

To further assess the effect of p53 activation on cellular levels of IL17RB, additional p53-activating agents were tested. As shown in Figure 2A, doxorubicin similarly reduced IL17RB levels in a dose-dependent manner. Etoposide (15 μM) and actinomycin D (5 nM) also reduced IL17RB levels (Figure 2B). Doses were selected based on prior studies demonstrating robust p53 stabilization without significant cytotoxicity after 24 h in LNCaP cells [37–39]. Notably, p53 levels did not consistently correlate inversely with IL17RB levels across different stimulus conditions, suggesting that additional p53-independent and/or stress-specific regulatory mechanisms contribute to IL17RB repression.

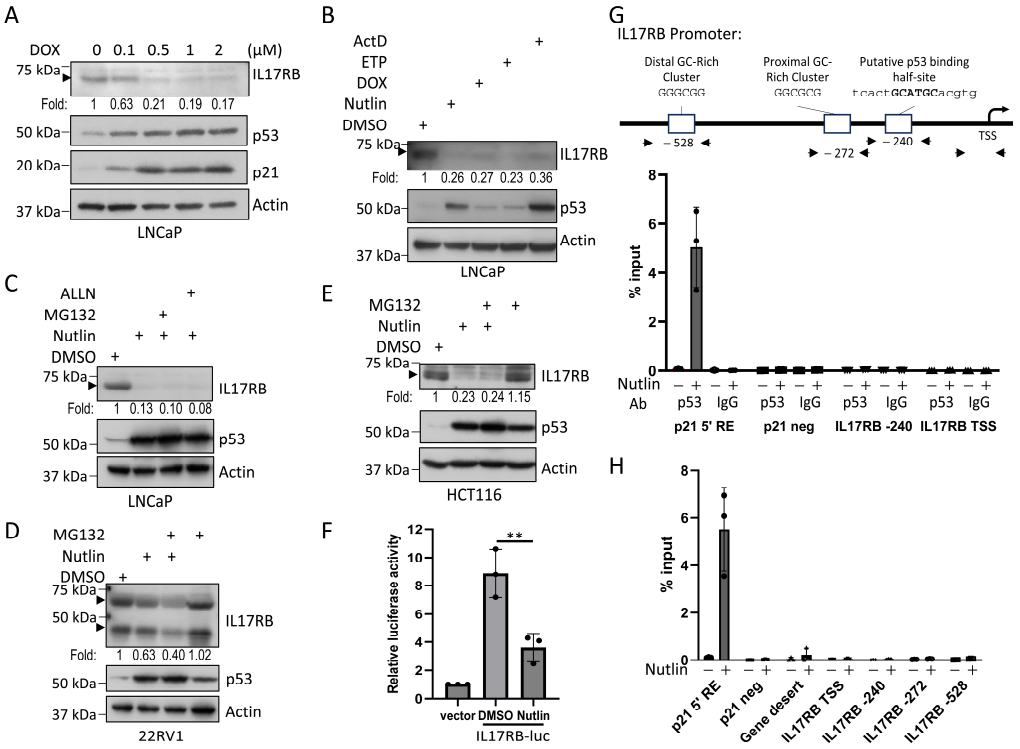


Figure 2. Nutlin-3a-induced p53 activation indirectly represses IL17RB expression. (**A**) Western blot analysis of LNCaP cells treated with increasing dosages of doxorubicin (Dox; 0, 0.1, 0.5, 1, or 2 μM) for 24 h. The arrow indicates full-length IL17RB. (**B**) Western blot analysis of LNCaP cells treated with DMSO, nutlin-3a (10 μM), Dox (doxorubicin; 1 μM), ETP (etoposide; 15 μM), or ActD (actinomycin D; 5 nM) for 24 h. The arrow indicates full-length IL17RB. (C-D) LNCaP (**C**), 22RV1 (**D**), and HCT116 (**E**) cells were treated with DMSO or nutlin-3a (10 μM) for 18 h, followed by the addition of the proteasome inhibitors MG132 (25 μM) or ALLN (20 μM) as indicated for 6 h. The arrow indicates full-length IL17RB. For 22RV1 cells, the bottom arrow indicates the faster-migrating species of IL17RB. (**F**) LNCaP cells were transfected with the pRL luciferase vector alone or together with the IL17RB-luc construct. Twenty-four hours after transfection, the IL17RB-luc-transfected cells were treated with DMSO or nutlin-3a (10 μM) for 24 h. Relative luciferase activity of IL17RB-luc was measured with the Duo-Glo luciferase assay system (n = 3; ** p < 0.01). (**G**,**H**) LNCaP cells were treated with DMSO or nutlin-3a (10 μM) for 24 h, followed by chromatin immunoprecipitation (ChIP) assays to assess p53 binding at the IL17RB promoter. A schematic of the IL17RB locus highlights a putative p53 half-site and two GC-rich regions (distal and proximal), along with the positions of the ChIP–qPCR primers (**G**). Normal IgG or anti-p53 (DO-1) antibody was used in (**G**), and

anti-p53 (DO-1) antibody was used in (**H**). Quantification of the IL17RB immunoblots was performed using ImageJ software. Fold: Relative full-length IL17RB amount.

To investigate the mechanism behind the nutlin-3a-induced reduction in IL17RB, we evaluated the role of protein turnover by treating cells with the proteasome inhibitors MG132 and ALLN. We found that both inhibitors failed to rescue the nutlin-3a-induced reduction in IL17RB in LNCaP (Figure 2C). Similarly, MG-132 did not rescue the effect of nutlin-3a on IL17RB in 22RV1 (Figure 2D) or HCT116 cells (Figure 2E). These data demonstrated that nutlin-3a reduces IL17RB levels through a proteasome-independent pathway. In addition, we performed an IL17RB promoter luciferase reporter assay. As shown in Figure 2F, nutlin-3a treatment significantly inhibited IL17RB promoter activity in LNCaP cells. Together with the RT-qPCR analysis shown in Figure 1, these data indicated that nutlin-3a downregulates IL17RB expression at the transcriptional level.

A putative half-site (−240) containing the core p53 binding motif (CWWG) was identified upstream of the IL17RB transcription start site (TSS). In addition, two GC-rich regions that may bind transcription factors were noted: a distal GC-rich cluster (−528) containing a canonical GGGCGG (Sp1) motif, and a proximal GC-rich cluster (−272) located near the putative p53 site. To determine whether p53 represses IL17RB directly or indirectly, we performed chromatin immunoprecipitation (ChIP) assays. As shown in Figure 2G,H, ChIP with an anti-p53 antibody followed by quantitative PCR detected robust p53 occupancy at the 5′ response element (5′RE) of the p21 promoter in nutlin-3a-treated LNCaP cells, serving as a positive control. In contrast, no significant p53 binding was observed at a distal region of the p21 gene or within a gene desert on chromosome 4, which served as negative controls. No p53 binding to the putative IL17RB half-site or the TSS region was detected, regardless of nutlin-3a treatment (Figure 2G). ChIP-qPCR targeting the two GC-rich clusters also showed no p53 recruitment (Figure 2H). These results indicated that p53 indirectly represses IL17RB.

3.2. Depletion of p53 or p21 Partially Rescues Nutlin-3a-Mediated IL17RB Reduction

To confirm the role of p53 in IL17RB repression, we depleted p53 using siRNAs. p53 knockdown partially rescued IL17RB expression in nutlin-3a-treated LNCaP cells, as shown by Western blot (Figure 3A) and quantitative RT-PCR (Figure 3B). A similar rescue was observed in HCT116 (Figure 3C) and U2OS (Figure S1) cells following p53 depletion, consistent with our observation that nutlin-3a-mediated IL17RB reduction occurred in HCT116 p53 +/+ but not p53 −/− cells (Figure 1H). In addition, doxorubicin-induced IL17RB reduction was partially reversed by p53 depletion in LNCaP cells, as was that of nutlin-3a (Figure 3A).

It has been well established that p21 is a major mediator of p53-dependent indirect repression [40–43]. To assess the role of p21 in IL17RB regulation, LNCaP cells were transfected with siRNAs targeting p21 and treated 24 h later with nutlin-3a or doxorubicin for an additional 24 h. As shown in Figure 3D,E, p21 knockdown partially rescued nutlin-3a- or doxorubicin-induced downregulation of IL17RB at both the protein and mRNA levels. Similarly, p21 depletion partially restored IL17RB expression in nutlin-3a-treated HCT116 cells (Figure 3F). Consistently, in HCT116 p21 −/− cells, nutlin-3a had little effect on IL17RB levels (Figure 3G). These findings support the established model of p21 as a major mediator of p53-dependent gene silencing. However, it has been reported that p53 could exert its repressive effects independent of p21 [44–46]. Further studies are needed to determine whether those p21-independent mechanisms are also responsible for IL17RB repression.

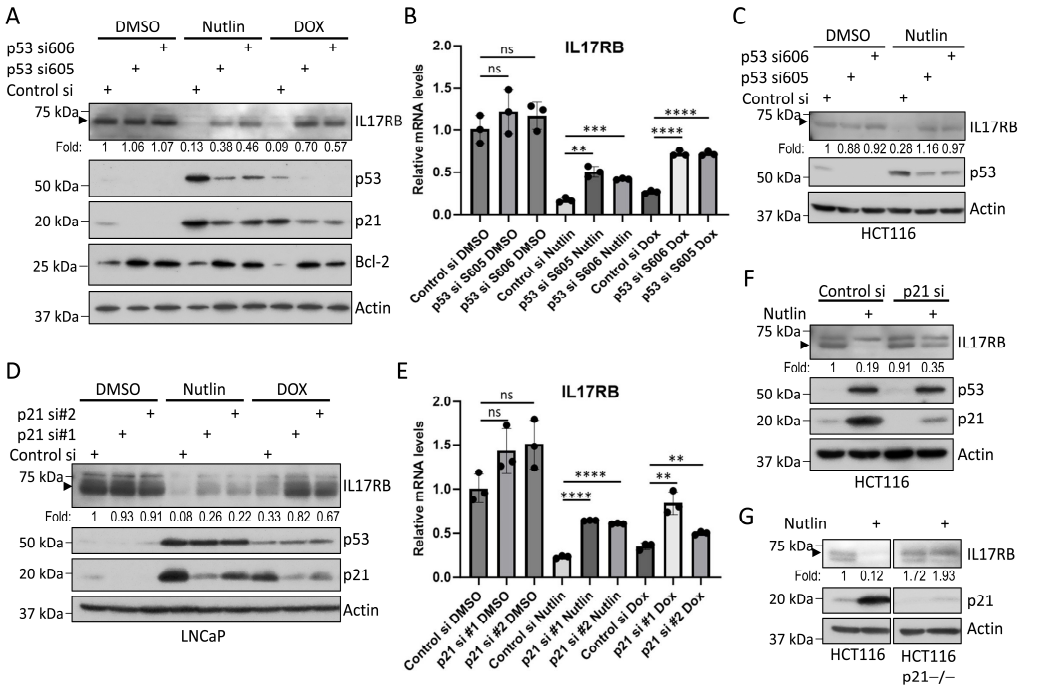


Figure 3. Depletion of p53 or p21 partially rescues the reduction in IL17RB induced by nutlin-3a. (**A**,**B**) LNCaP cells were transfected with control siRNA or two siRNAs targeting p53 (si605 and si606). Twenty-four hours after transfection, the cells were treated with DMSO, nutlin-3a (10 μM), or Dox (doxorubicin; 1 μM) for 24 h. The cells were harvested and subjected to Western blot analysis (**A**) or qRT-PCR analysis (**B**). Data were presented as mean ± SE (n = 3; ** $p < 0.01$; *** $p < 0.001$; **** $p < 0.0001$). (**C**) HCT116 cells were transfected with control siRNA or siRNAs targeting p53 (si605 and si606) and treated with DMSO or nutlin-3a (10 μM) for 24 h, followed by Western blot analysis. (**D**,**E**) LNCaP cells were transfected with control siRNA or two siRNAs targeting p21 (#1 and #2). Twenty-four hours after transfection, the cells were treated with DMSO, nutlin-3a (10 μM), or Dox (doxorubicin; 1 μM) for 24 h. The cells were harvested and subjected to Western blot analysis (**D**) or qRT-PCR analysis (**E**). (**F**) HCT116 cells were transfected with control siRNA or siRNAs targeting p21 (#1 and #2) and treated as described in (**C**), followed by Western blot analysis. (**G**) HCT116 and HCT116 p21 −/− cells were treated with DMSO or nutlin-3a (10 μM) for 24 h. The cells were harvested and subjected to Western blot analysis. The arrow indicates full-length IL17RB. Fold: Relative full-length IL17RB amount.

3.3. IL17RB Regulates Nutlin-3a-Induced Cell Growth and Cell Migration Inhibition by Modulating Cellular Levels of p21 and Bcl-2

To assess the physiological effects of IL17RB repression and IL17RB overexpression, we transfected LNCaP, HCT116, or U2OS cells with siRNAs targeting IL17RB or the CMV-IL17RB plasmid and examined cellular outcomes using various assays. As shown in Figure 4A, LNCaP cells depleted of IL17RB showed reduced proliferation and were more sensitive to nutlin-3a treatment than control siRNA-treated cells. Moreover, LNCaP cells with p53 and IL17RB co-depletion exhibited reduced cell proliferation compared to LNCaP cells treated with siRNAs targeting p53 alone with or without the presence of nutlin-3a (Figure 4B). Similarly, IL17RB knockdown in HCT116 p53 +/+ cells reduced cell proliferation and increased sensitivity to nutlin-3a treatment. In contrast, HCT116 p53 −/− cells were resistant to nutlin-3a, and IL17RB depletion reduced cell proliferation regardless of nutlin-3a treatment (Figure 4C). On the other hand, HCT116 cells with IL17RB overexpression were more resistant to nutlin-3a treatment than HCT116 cells without IL17RB overexpression in colony formation assays (Figure 4D). In a transwell migration assay, we observed that IL17RB overexpression promoted the migration of

U2OS cells treated with nutlin-3a (Figure 4E). Collectively, these data indicated that cellular levels of IL17RB regulate nutlin-3a-induced inhibition of cell growth and migration.

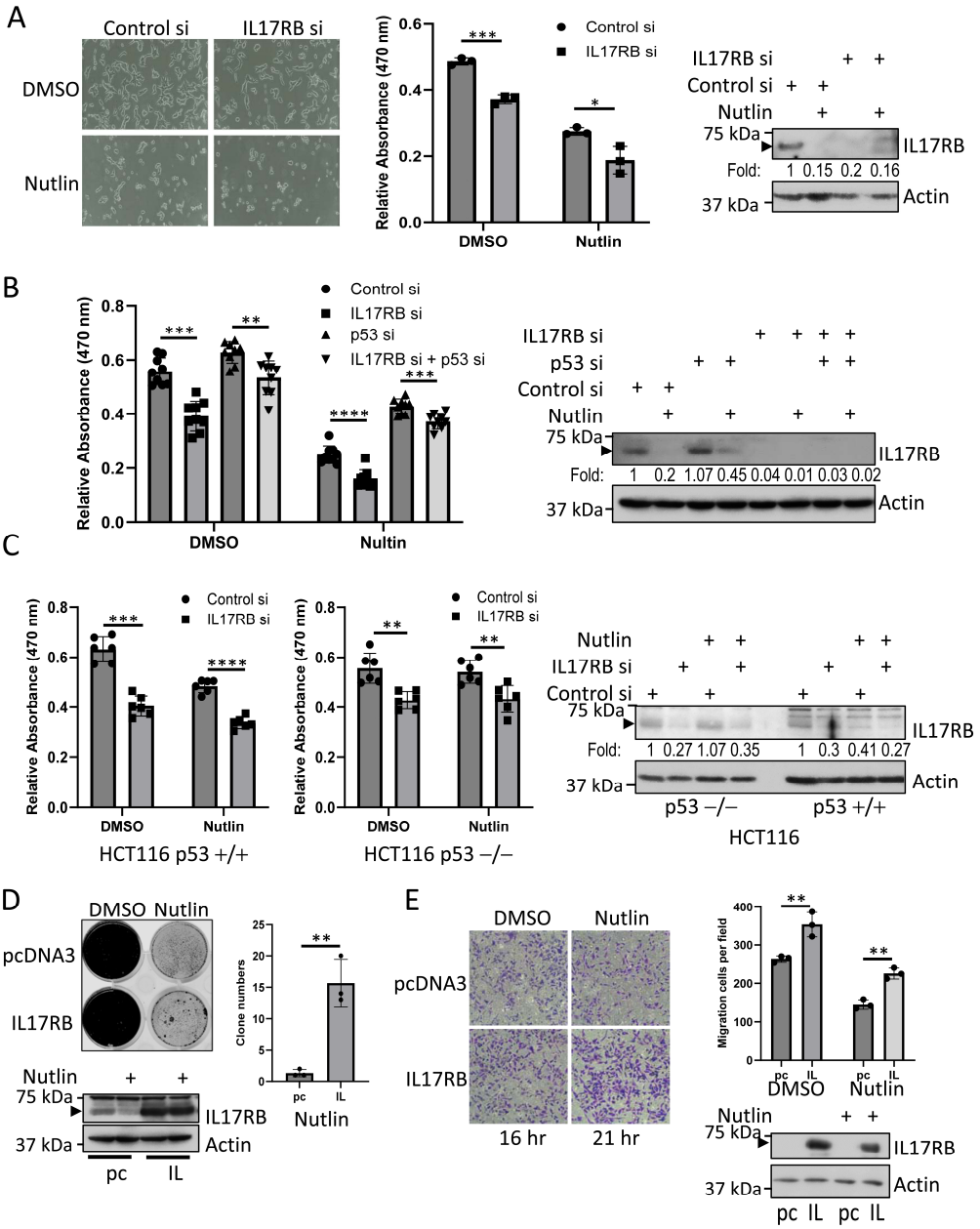


Figure 4. IL17RB Expression Modulates nutlin-3a-induced inhibition of cell growth and cell migration. (**A**) IL17RB depletion enhances nutlin-3a-induced cell growth inhibition. Left Panel: Visualizations of LNCaP cells transfected with control siRNA or a pool of siRNAs targeting IL17RB for 24 h, followed by another 24 h with DMSO or nutlin-3a (10 μM) treatment. Middle Panel: Cell proliferation analysis of LNCaP cells that were transfected with control siRNA or a pool of siRNAs targeting IL17RB for 24 h, followed by another 24 h with DMSO or nutlin-3a (10 μM) treatment (n = 3; * p < 0.05; *** p < 0.001). Right Panel: Western Blot analysis confirming the effective knockdown of IL17RB. (**B**) Cell proliferation analysis of LNCaP cells that were transfected with control siRNA, a pool of siRNAs targeting IL17RB, a pool of siRNA targeting p53, or a combination of siRNAs targeting both IL17RB and p53 for 24 h, followed by another 24 h with DMSO or nutlin-3a (10 μM) treatment (n = 9; ** p < 0.01; *** p < 0.001; **** p < 0.0001). Right Panel: Western Blot analysis confirming the effective knockdown of IL17RB. (**C**) Cell proliferation analysis of HCT116 (p53 +/+ or p53 −/−) cells that were transfected with control siRNA or a pool of siRNAs targeting IL17RB for 24 h, followed by another

24 h with DMSO or nutlin-3a (10 μM) treatment ($n = 6$; ** $p < 0.01$; *** $p < 0.001$; **** $p < 0.0001$). (**D**) HCT116 cells with IL17RB overexpression are more resistant to nutlin-3a treatment. Left Panel: $1X10^4$ HCT116 cells transfected with pcDNA3 or cmv-IL17RB were plated, treated with 10 μM nutlin-3a for 14 days, then fixed and stained with crystal violet. Fresh media were replaced every other day. A representative image was shown. Western blot analysis confirming the effective overexpression of IL17RB in HCT116 cells is also shown. Right Panel: Clone numbers for nutlin-3a-treated cells were counted and plotted from three independent experiments with GraphPad Prism ($n = 3$; ** $p < 0.01$). (**E**) IL17RB overexpression promotes nutlin-3a-treated U2OS migration. $3X10^4$ U2OS cells transfected with pcDNA3 or cmv-IL17RB were resuspended in serum-free DMEM medium containing DMSO or 10 μM nutlin-3a and seeded in the upper chamber of the 24-well Transwell insert. DMEM with 2%FBS was used as an attractant in the lower chamber. Migrated cells were fixed and stained at 16 h for DMSO-treated cells and 21 h for nutlin-3a-treated cells. A representative image was shown (Left panel). Cell counts for Transwell migration in randomly selected view fields were graphed (Right panel; $n = 3$; ** $p < 0.01$). Western Blot analysis confirming the effective overexpression of IL17RB in U2OS cells was also shown. The arrow indicates full-length IL17RB. Fold: Relative full-length IL17RB amount.

It has been shown that IL17B, a ligand of IL17RB, binds to IL17RB, activating signaling pathways that upregulate the expression of anti-apoptotic protein Bcl-2 [19,26,47]. We treated LNCaP or HCT116 cells in the presence or absence of IL17B and found that nutlin-3a-mediated p21 induction and Bcl-2 repression were compromised upon IL17B incubation (Figure 5A,B). The observed effects of IL17B on p21 and Bcl-2 were attenuated upon IL17RB depletion, suggesting they are specifically mediated by IL17RB (Figure 5C). In addition, Western blot analysis of LNCaP (Figure 5D) or HCT116 (Figure 5E) cells revealed that IL17RB depletion enhances, while IL17RB overexpression reduces nutlin-3a-induced p21 expression (Figure 5F). Together, our data implied that p53-mediated repression of IL17RB may sustain the p53 response by modulating cellular levels of p21 and Bcl-2, thereby contributing to p53's tumor-suppressive function.

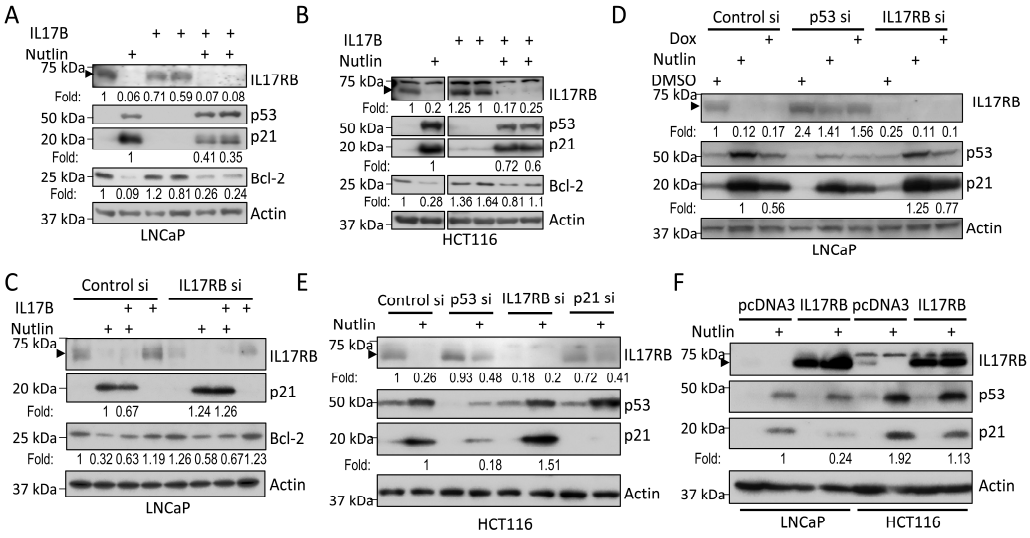


Figure 5. IL17B treatment counteracts nutlin-3a-mediated p21 induction and Bcl-2 repression. LNCaP cells (**A**) or HCT116 cells (**B**) were treated as indicated with DMSO or nutlin-3a (10 μM) in the absence or presence of IL17B (50 ng/mL) for 24 h. The cells were harvested and subjected to Western blot analysis. IL17RB depletion enhances nutlin-3a or doxorubicin-induced p21 expression. (**C**) LNCaP cells were transfected with control siRNA or a pool of siRNAs targeting IL17RB. Twenty-four hours after transfection, the cells were treated as indicated with DMSO or nutlin-3a (10 μM) in the absence or presence of IL17B (50 ng/mL) for 24 h. The cells were harvested and subjected to

Western blot analysis. (**D**) LNCaP cells were transfected with control siRNA, siRNAs targeting p53 (si605 and si606), or a pool of siRNAs targeting IL17RB. Twenty-four hours after transfection, the cells were treated with DMSO, nutlin-3a (10 μM), or Dox (doxorubicin; 1 μM) for 24 h. The cells were harvested and subjected to Western blot analysis. (**E**) HCT116 cells were transfected with control siRNA, siRNAs targeting p53 (si605 and si606), a pool of siRNAs targeting IL17RB, or siRNAs targeting p21 (#1 and #2). Twenty-four hours after transfection, the cells were treated with DMSO or nutlin-3a (10 μM) for 24 h. The cells were harvested and subjected to Western blot analysis. (**F**) IL17RB overexpression reduces nutlin-3a-induced p21 expression. LNCaP cells or HCT116 cells were transfected with pcDNA3 or cmv-IL17RB for 24 h, followed by another 24 h with DMSO or nutlin-3a (10 μM) treatment. The cells were harvested and subjected to Western blot analysis. Immunoblots are representative of at least two independent experiments. Quantification of immunoblots (IL17RB, A-E; p21, A-E; and Bcl-2, A-B) was performed using ImageJ software. The arrow indicates full-length IL17RB. Fold: Relative full-length IL17RB, p21, or Bcl-2 amount.

3.4. IL17RB Is Overexpressed in Prostate and Colon Cancer Samples

Our experimental data were obtained using LNCaP prostate cancer cells and HCT116 colon cancer cells. To determine whether IL17RB is clinically important in prostate and colon cancers, we compared IL17RB levels in normal and cancer samples with publicly available datasets from tnmplot.com. The Normal and Tumor analyses using RNA-Seq data from paired tumors or adjacent normal tissues for prostate and colon adenocarcinomas revealed that IL17RB levels are higher in cancer samples than in normal samples (Figure 6A). The Normal and Tumor analyses using gene chip-based data from paired (Figure S2A) or non-paired (Figure S2B) tumors or adjacent normal tissues for prostate and colon adenocarcinomas showed similar results. We also compared the levels of IL17RB in normal prostate gland to those in prostate carcinoma from two prostate cancer datasets in Oncomine.org (GSE3933 [32] and GSE21034 [33] datasets). As shown in Figure 6B, IL17RB is higher in prostate cancer samples than in the normal prostate gland. In addition, higher levels of IL17RB were observed in cancer samples across all stages compared with normal samples, as determined by stage-specific gene array analysis of prostate and colon tumor samples (Figure 6C). Furthermore, gene expression array analysis of colon tumor samples revealed a moderate but statistically significant positive correlation between IL17RB and Bcl-2, and a negative correlation with p21 (Figure 6D). In prostate tumor samples, IL17RB expression also showed a statistically significant positive correlation with Bcl-2 and a tendency toward an inverse correlation with p21, although the latter did not reach statistical significance (Figure 6E). These observations were in line with our data in Figure 5, in which IL17RB expression is associated with higher Bcl-2 and lower p21 levels.

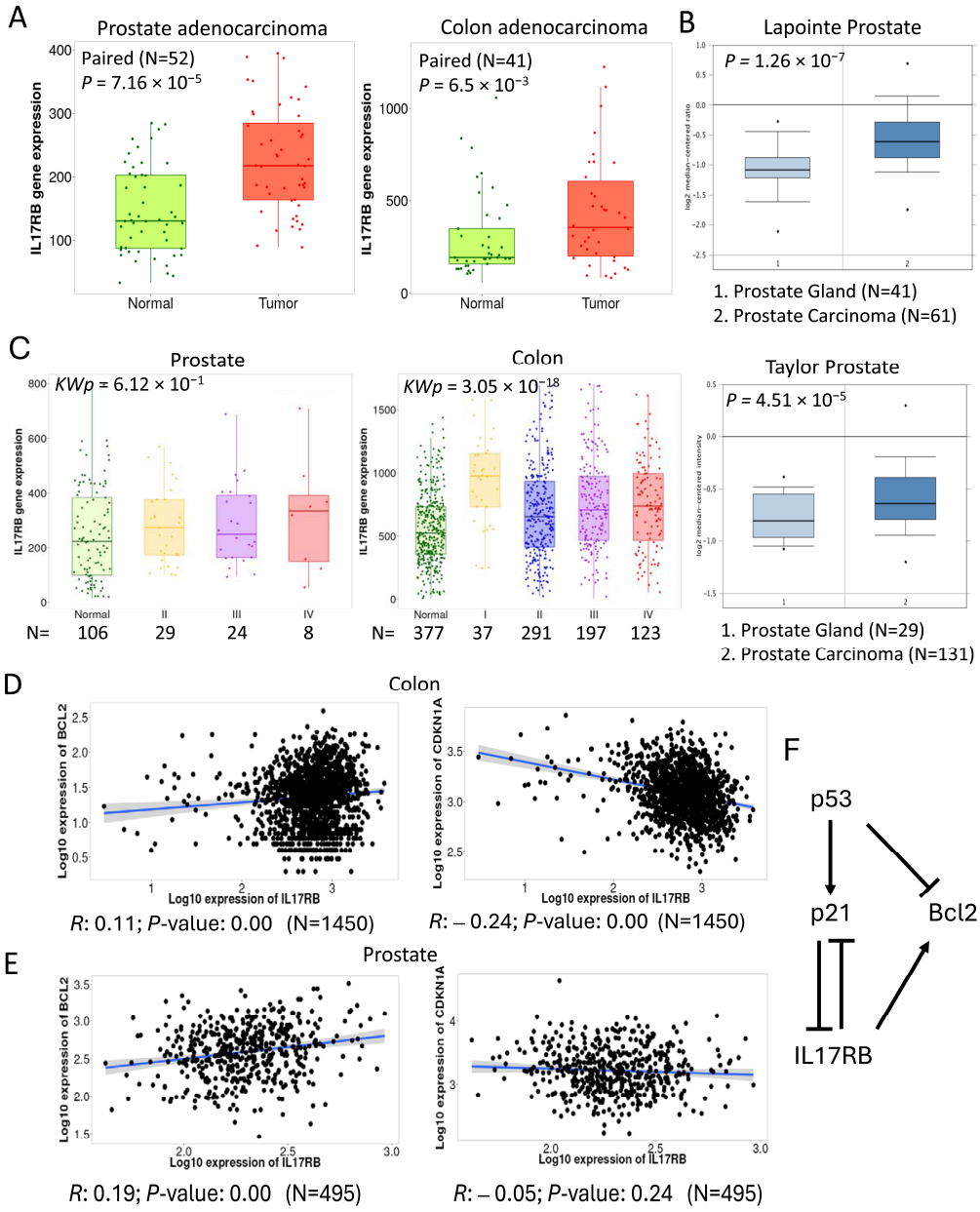


Figure 6. IL17RB is overexpressed in prostate and colon cancers. Levels of IL17RB mRNA in paired normal and tumor samples were retrieved from TNMplot.com by analyzing prostate adenocarcinoma and colon adenocarcinoma datasets (**A**). IL17RB mRNA levels in normal prostate gland and prostate carcinoma tissues were further compared using two independent prostate cancer datasets from Oncomine.com (**B**). Statistical significance (*p* values) in (**A**,**B**) was determined using the Mann–Whitney test. (**C**) Stage-specific analysis of IL17RB expression in prostate and colon cancers. Statistical significance was assessed using the Kruskal–Wallis test. (**D**) Spearman correlation analysis of IL17RB with Bcl-2 (left) and p21 (right) using gene expression array data from colon tumor samples. (**E**) Spearman correlation analysis of IL17RB with Bcl-2 (left) and p21 (right) using RNA-seq data from prostate tumor samples. (**F**) Schematic diagram illustrating a potential feedback loop within the p53-p21-IL17RB axis.

4. Discussion

IL17RB was identified as a gene strongly repressed by MDM2/MDMX inhibitors in a reanalysis of global gene expression data from a previous study using prostate cancer LNCaP cells [29]. We confirmed that nutlin-3a decreased IL17RB levels in several wild-type p53 cell lines, but not in mutant or p53-null cell lines, demonstrating that p53 is

required for nutlin-3a-mediated repression of IL17RB expression. Although quantitative RT-PCR and IL17RB promoter reporter assays demonstrated transcriptional repression of IL17RB, ChIP analysis failed to detect p53 binding to the IL17RB promoter in nutlin-3a-treated cells, suggesting that p53-mediated repression of IL17RB occurs indirectly. Depletion of either p53 or p21 partially rescued nutlin-3a-mediated IL17RB downregulation, consistent with the established model in which p21 contributes to p53-dependent gene repression, although p21-independent mechanisms cannot be ruled out. Given that p21 typically mediates transcriptional repression through the DREAM complex [42], RB-E2F signaling [41], or recruitment of specific co-repressors [48], further studies are needed to elucidate the mechanisms underlying IL17RB repression. Intriguingly, p53 levels did not consistently correlate inversely with IL17RB levels across treatment conditions, suggesting that the extent of IL17RB repression may also be influenced by additional stimulus- or context-dependent regulatory mechanisms. Future investigations are warranted to dissect these mechanisms and clarify their relative contributions to IL17RB repression.

Amplified IL17RB signaling has been shown to promote tumorigenesis in breast, gastric, lung, pancreatic, and thyroid cancers [26,27,48–50]. We also found that IL17RB is overexpressed in prostate and colon cancer samples in comparison to normal samples in multiple publicly available datasets. Those results supported the literature on IL17RB signaling as oncogenic and suggested that its repression may contribute to p53's tumor-suppressive function. To assess the biological outcome of p53-mediated IL17RB repression, we found that IL17RB depletion reduces cell proliferation and sensitizes cells to nutlin-3a treatment in wild-type p53-containing LNCaP and HCT116 cells. In LNCaP cells with p53 knockdown or in HCT116 p53 −/− cells, IL17RB depletion also reduces cell proliferation but does not respond to nutlin-3a treatment. On the other hand, IL17RB overexpression renders cells more resistant to nutlin-3a in colony formation assays. Due to the limited migratory capacity of LNCaP cells, we were unable to assess their behavior in migration assays. In HCT116 cells, we have not yet obtained conclusive evidence regarding the effect of IL17RB overexpression on cell migration. In U2OS osteosarcoma cells overexpressing IL17RB, we observed enhanced migration. It is possible that IL17RB promotes migration in a cell-type-dependent manner. Notably, we found that HCT116 cells express relatively high basal levels of IL17RB compared to U2OS cells, with expression levels comparable to those achieved in U2OS cells upon IL17RB overexpression (Figure S3). It is therefore plausible that endogenous IL17RB levels in HCT116 cells are already sufficient to promote migration, and additional ectopic IL17RB expression does not further enhance this phenotype. Future studies are warranted to investigate the effects of IL17RB signaling on other p53-mediated cellular responses beyond its roles in regulating cell proliferation and migration.

Intriguingly, IL17RB knockdown was associated with enhanced nutlin-3a-induced p21 expression, suggesting a potential feedback relationship within the p53-p21-IL17RB axis (Figure 6F). Several cancer-prone signaling pathways have been reported to mediate the oncogenic function of IL17RB [16–19]. One notable mechanism involved is the upregulation of anti-apoptotic factor Bcl-2 with amplified IL17RB signaling [19,26,47]. We observed that IL17B, an IL17RB ligand that was shown to activate IL17RB signaling in multiple cancers [20], partially counteracted nutlin-3a-induced Bcl-2 repression. Nutlin-3a-mediated p21 induction and Bcl-2 repression were compromised upon IL17B incubation in control siRNA-treated cells but not in IL17RB siRNA-treated cells, suggesting that the effect of IL17B is mediated by IL17RB. However, IL17RB knockdown did not affect cellular Bcl-2 levels in the absence of IL17B, implying that IL17RB-mediated regulation of Bcl-2 is ligand-dependent. Bioinformatic analysis further showed a moderate positive correlation between IL17RB and Bcl-2 expression in both colon and prostate tumors. Collectively, these findings suggest that interactions between p53 pathway activity and IL17B/IL17RB

signaling may influence cell fate involving p21 and Bcl-2. Further studies will be required to define the signaling pathways downstream of IL17RB that intersect with p53 signaling.

Despite the reported oncogenic properties of IL17RB signaling, the prognostic value of IL17RB seemed to vary by cancer type. It has been documented that high IL17RB expression correlates with reduced overall survival or disease-free survival in pancreatic, breast, lung, gastric, and oral squamous cell carcinoma cancer patients [20]. However, reports suggested that IL17RB may be a good prognostic marker, as the HOXB13/IL17RB expression ratio was associated with better clinical outcomes in early-stage estrogen receptor-positive/lymph node-positive breast cancer after adjuvant tamoxifen monotherapy [51,52]. Additionally, a recent study showed that IL17B gene and protein expression levels decreased, while IL17RB expression increased in colorectal cancer (CRC), and that high IL17RB levels were associated with improved overall survival and immune cell infiltration [53]. Our stage analysis of gene array data showed that stage I cancers had higher IL17RB levels than those in stages II, III, and IV, and that IL17RB levels were higher in cancer samples across all stages compared with normal colon tissue. These observations suggested a potential stage-dependent association among IL17B and IL17RB expression, p53 pathway status, and tumor immune context. IL17RB signaling may act as a double-edged sword depending on the duration of stress and the tumor's evolutionary stage, as has been shown for macrophage inhibitory cytokine 1 (MIC-1). MIC-1 signaling is not only an anti-inflammatory modulator but also a potent immunosuppressive enhancer by superinducing proinflammatory chemokines in chronic inflammatory states, in a cell-context- and tumor-stage-dependent manner [54–56]. Additionally, IL25 (also known as IL17E), is another ligand for IL17RB [16]. It has been documented that IL-25 binds to the IL17RA/IL17RB receptor complex, initiating and maintaining type 2 immunity, and regulating other immune cells [57–62]. It has also been shown that IL-25 exhibits an anti-cancer effect [26,63], inducing caspase-mediated apoptosis in breast cancer cells and reducing the growth of breast tumor xenografts in vivo. It may contribute to the tissue- and tumor-type-dependent, as well as stage-dependent, biological functions of IL17RB. Given our identified link between p53 and IL17RB, it will also be of interest to investigate whether p53 influences inflammation and immune responses by modulating IL17RB signaling in future studies.

5. Conclusion

In this study, we demonstrated that p53 is required for nutlin-3a-mediated repression of IL17RB expression. p53-mediated repression of IL17RB most likely occurs indirectly via p21, although the molecular mechanism underlying p53-dependent repression of IL17RB remains insufficiently elucidated. We observed that IL17RB depletion enhances, whereas overexpression attenuates, nutlin-3a-induced inhibition of cell proliferation and migration, as well as nutlin-3a-induced p21 expression. IL17B treatment decreases nutlin-3a-induced p21 induction and Bcl-2 repression. Although there is no evidence of a causal relationship, IL17RB is elevated in prostate/colon tumors and shows a moderate positive correlation with Bcl-2 and a negative correlation with p21 in colon tumors. These findings suggest a potential feedback relationship within the p53-p21-IL17RB axis and the contribution of p53-mediated IL17RB repression in tumor suppression.

Supplementary Materials: The following supporting information can be downloaded at https://www.mdpi.com/article/10.3390/cells15222066/s1. Figure S1: Depletion of p53 rescues nutlin-3a-mediated reduction in IL17RB in U2OS cells; Figure S2: IL17RB is overexpressed in prostate and colon cancers; Figure S3: HCT116 cells have higher levels of endogenous IL17RB compared to U2OS cells. Figure S4. Densitometric quantification of relative IL17RB levels from independent Western blot experiments in Figure 1. Figure S5. Densitometric quantification of relative IL17RB levels from

independent Western blot experiments in Figure 2. Figure S6. Densitometric quantification of relative IL17RB levels from independent Western blot experiments in Figure 3. Figure S7. Densitometric quantification of relative p21 or Bcl-2 levels from independent Western blot experiments in Figure 5.

Author Contributions: A.P., C.S., and Y.Z. data curation; S.S. and Y. Z. validation; A.P., C.S., S.S., J.S., O.H., and Y.Z. investigation; C.S., S.S., J.S., O.H., I.V., and Y.Z. methodology; A.P., Y.Z. and I.V. writing, review, and editing; Y.Z. and I.V. resources; Y.Z. conceptualization; Y.Z. supervision; Y.Z. funding acquisition; Y.Z. project administration. All authors have read and agreed to the published version of the manuscript.

Funding: This study was supported by the US National Cancer Institute (NCI) of the National Institutes of Health (NIH), grant number R15CA287406 (to Y.Z.). The content is solely the responsibility of the authors and does not necessarily represent the official views of the NIH. The APC was funded by grant number R15CA287406.

Institutional Review Board Statement: Not applicable.

Data Availability Statement: The integrated datasets analyzed via TNMplot platform are originally derived from public repositories including TCGA, TARGET, GTEx, and NCBI GEO, as described in Bartha & Győrffy (2021) [34]. The datasets GSE3933 and GSE21034 are available in the Gene Expression Omnibus (GEO). All other data are contained within the manuscript.

Acknowledgments: Thanks to Carol Prives and Elzbieta Freulich for sharing multiple cell lines.

Conflicts of Interest: The authors declare no conflicts of interest.

References

1. Vogelstein, B.; Lane, D.; Levine, A.J. Surfing the p53 network. *Nature* **2000**, *408*, 307–310. https://doi.org/10.1038/35042675.
2. Olivier, M.; Hollstein, M.; Hainaut, P. *TP53* mutations in human cancers: Origins, consequences, and clinical use. *Cold Spring Harb. Perspect. Biol.* **2010**, *2*, a001008. https://doi.org/10.1101/cshperspect.a001008.
3. Rivlin, N.; Brosh, R.; Oren, M.; Rotter, V. Mutations in the p53 Tumor Suppressor Gene: Important Milestones at the Various Steps of Tumorigenesis. *Genes Cancer* **2011**, *2*, 466–474. https://doi.org/10.1177/1947601911408889.
4. Oren, M.; Prives, C. p53: A tale of complexity and context. *Cell* **2024**, *187*, 1569–1573. https://doi.org/10.1016/j.cell.2024.02.043.
5. Liu, Y.; Su, Z.; Tavana, O.; Gu, W. Understanding the complexity of p53 in a new era of tumor suppression. *Cancer Cell* **2024**, *42*, 946–967. https://doi.org/10.1016/j.ccell.2024.04.009.
6. Shi, D.; Jiang, P. A Different Facet of p53 Function: Regulation of Immunity and Inflammation During Tumor Development. *Front. Cell Dev. Biol.* **2021**, *9*, 762651. https://doi.org/10.3389/fcell.2021.762651.
7. Levine, A.J. P53 and The Immune Response: 40 Years of Exploration-A Plan for the Future. *Int. J. Mol. Sci.* **2020**, *21*, 541. https://doi.org/10.3390/ijms21020541.
8. Vousden, K.H.; Lu, X. Live or let die: The cell's response to p53. *Nat. Rev. Cancer* **2002**, *2*, 594–604. https://doi.org/10.1038/nrc864.
9. Chen, J. The Cell-Cycle Arrest and Apoptotic Functions of p53 in Tumor Initiation and Progression. *Cold Spring Harb. Perspect. Med.* **2016**, *6*, a026104. https://doi.org/10.1101/cshperspect.a026104.
10. Gudkov, A.V.; Gurova, K.V.; Komarova, E.A. Inflammation and p53: A Tale of Two Stresses. *Genes Cancer* **2011**, *2*, 503–516. https://doi.org/10.1177/1947601911409747.
11. Cooks, T.; Harris, C.C.; Oren, M. Caught in the cross fire: p53 in inflammation. *Carcinogenesis* **2014**, *35*, 1680–1690. https://doi.org/10.1093/carcin/bgu134.
12. Wu, H.H.; Leng, S.; Eisenstat, D.D.; Sergi, C.; Leng, R. Targeting p53 for immune modulation: Exploring its functions in tumor immunity and inflammation. *Cancer Lett.* **2025**, *617*, 217614. https://doi.org/10.1016/j.canlet.2025.217614.
13. McGeachy, M.J.; Cua, D.J.; Gaffen, S.L. The IL-17 Family of Cytokines in Health and Disease. *Immunity* **2019**, *50*, 892–906. https://doi.org/10.1016/j.immuni.2019.03.021.
14. Monin, L.; Gaffen, S.L. Interleukin 17 Family Cytokines: Signaling Mechanisms, Biological Activities, and Therapeutic Implications. *Cold Spring Harb. Perspect. Biol.* **2018**, *10*, a028522. https://doi.org/10.1101/cshperspect.a028522.
15. Gaffen, S.L. Structure and signalling in the IL-17 receptor family. *Nat. Rev. Immunol.* **2009**, *9*, 556–567. Erratum in *Nat. Rev. Immunol.* **2009**, *9*, 747. https://doi.org/10.1038/nri2586.

16. Lee, J.; Ho, W.H.; Maruoka, M.; Corpuz, R.T.; Baldwin, D.T.; Foster, J.S.; Goddard, A.D.; Yansura, D.G.; Vandlen, R.L.; Wood, W.I.; et al. IL-17E, a novel proinflammatory ligand for the IL-17 receptor homolog IL-17Rh1. *J. Biol. Chem.* **2001**, *276*, 1660–1664. https://doi.org/10.1074/jbc.M008289200.
17. Maezawa, Y.; Nakajima, H.; Suzuki, K.; Tamachi, T.; Ikeda, K.; Inoue, J.; Saito, Y.; Iwamoto, I. Involvement of TNF receptor-associated factor 6 in IL-25 receptor signaling. *J. Immunol.* **2006**, *176*, 1013–1018. https://doi.org/10.4049/jimmunol.176.2.1013.
18. Wong, C.K.; Cheung, P.F.; Ip, W.K.; Lam, C.W. Interleukin-25-induced chemokines and interleukin-6 release from eosinophils is mediated by p38 mitogen-activated protein kinase, c-Jun N-terminal kinase, and nuclear factor-kappaB. *Am. J. Respir. Cell Mol. Biol.* **2005**, *33*, 186–194. https://doi.org/10.1165/rcmb.2005-0034OC.
19. Laprevotte, E.; Cochaud, S.; du Manoir, S.; Lapierre, M.; Dejou, C.; Philippe, M.; Giustiniani, J.; Frewer, K.A.; Sanders, A.J.; Jiang, W.G.; et al. The IL-17B-IL-17 receptor B pathway promotes resistance to paclitaxel in breast tumors through activation of the ERK1/2 pathway. *Oncotarget* **2017**, *8*, 113360–113372. https://doi.org/10.18632/oncotarget.23008.
20. Bastid, J.; Dejou, C.; Docquier, A.; Bonnefoy, N. The Emerging Role of the IL-17B/IL-17RB Pathway in Cancer. *Front. Immunol.* **2020**, *11*, 718. https://doi.org/10.3389/fimmu.2020.00718.
21. Bie, Q.; Song, H.; Chen, X.; Yang, X.; Shi, S.; Zhang, L.; Zhao, R.; Wei, L.; Zhang, B.; Xiong, H. IL-17B/IL-17RB signaling cascade contributes to self-renewal and tumorigenesis of cancer stem cells by regulating *Beclin-1* ubiquitination. *Oncogene* **2021**, *40*, 2200–2216. https://doi.org/10.1038/s41388-021-01699-4.
22. Lavorgna, A.; Matsuoka, M.; Harhaj, E.W. A critical role for IL-17RB signaling in HTLV-1 tax-induced NF-κB activation and T-cell transformation. *PLoS Pathog.* **2014**, *10*, e1004418. https://doi.org/10.1371/journal.ppat.1004418.
23. Guo, H.Z.; Niu, L.T.; Qiang, W.T.; Chen, J.; Wang, J.; Yang, H.; Zhang, W.; Zhu, J.; Yu, S.H. Leukemic IL-17RB signaling regulates leukemic survival and chemoresistance. *FASEB J.* **2019**, *33*, 9565–9576. https://doi.org/10.1096/fj.201900099R.
24. Bie, Q.; Jin, C.; Zhang, B.; Dong, H. IL-17B: A new area of study in the IL-17 family. *Mol. Immunol.* **2017**, *90*, 50–56. https://doi.org/10.1016/j.molimm.2017.07.004.
25. Alinejad, V.; Dolati, S.; Motallebnezhad, M.; Yousefi, M. The role of IL17B-IL17RB signaling pathway in breast cancer. *Biomed. Pharmacother.* **2017**, *88*, 795–803. https://doi.org/10.1016/j.biopha.2017.01.120.
26. Huang, C.K.; Yang, C.Y.; Jeng, Y.M.; Chen, C.L.; Wu, H.H.; Chang, Y.C.; Ma, C.; Kuo, W.H.; Chang, K.J.; Shew, J.Y.; et al. Autocrine/paracrine mechanism of interleukin-17B receptor promotes breast tumorigenesis through NF-κB-mediated antiapoptotic pathway. *Oncogene* **2014**, *33*, 2968–2977. https://doi.org/10.1038/onc.2013.268.
27. Wu, H.H.; Hwang-Verslues, W.W.; Lee, W.H.; Huang, C.K.; Wei, P.C.; Chen, C.L.; Shew, J.Y.; Lee, E.Y.; Jeng, Y.M.; Tien, Y.W.; et al. Targeting IL-17B-IL-17RB signaling with an anti-IL-17RB antibody blocks pancreatic cancer metastasis by silencing multiple chemokines. *J. Exp. Med.* **2015**, *212*, 333–349. https://doi.org/10.1084/jem.20141702.
28. Gudkov, A.V.; Komarova, E.A. p53 and the Carcinogenicity of Chronic Inflammation. *Cold Spring Harb. Perspect. Med.* **2016**, *6*, a026161. https://doi.org/10.1101/cshperspect.a026161.
29. Chopra, H.; Khan, Z.; Contreras, J.; Wang, H.; Sedrak, A.; Zhu, Y. Activation of p53 and destabilization of androgen receptor by combinatorial inhibition of *MDM2* and *MDMX* in prostate cancer cells. *Oncotarget* **2018**, *9*, 6270–6281. https://doi.org/10.18632/oncotarget.23569.
30. Singer, S.; Zhao, R.; Barsotti, A.M.; Ouwehand, A.; Fazollahi, M.; Coutavas, E.; Breuhahn, K.; Neumann, O.; Longerich, T.; Pusterla, T.; et al. Nuclear pore component *Nup98* is a potential tumor suppressor and regulates posttranscriptional expression of select p53 target genes. *Mol. Cell* **2012**, *48*, 799–810. https://doi.org/10.1016/j.molcel.2012.09.020.
31. Moon, S.H.; Huang, C.H.; Houlihan, S.L.; Regunath, K.; Freed-Pastor, W.A.; Morris, J.P.; Tschaharganeh, D.F.; Kastenhuber, E.R.; Barsotti, A.M.; Culp-Hill, R.; et al. p53 Represses the Mevalonate Pathway to Mediate Tumor Suppression. *Cell* **2019**, *176*, 564–580.e519. https://doi.org/10.1016/j.cell.2018.11.011.
32. Lapointe, J.; Li, C.; Higgins, J.P.; van de Rijn, M.; Bair, E.; Montgomery, K.; Ferrari, M.; Egevad, L.; Rayford, W.; Bergerheim, U.; et al. Gene expression profiling identifies clinically relevant subtypes of prostate cancer. *Proc. Natl. Acad. Sci. USA* **2004**, *101*, 811–816. https://doi.org/10.1073/pnas.0304146101.
33. Taylor, B.S.; Schultz, N.; Hieronymus, H.; Gopalan, A.; Xiao, Y.; Carver, B.S.; Arora, V.K.; Kaushik, P.; Cerami, E.; Reva, B.; et al. Integrative genomic profiling of human prostate cancer. *Cancer Cell* **2010**, *18*, 11–22. https://doi.org/10.1016/j.ccr.2010.05.026.
34. Bartha, Á.; Győrffy, B. TNMplot.com: A Web Tool for the Comparison of Gene Expression in Normal, Tumor and Metastatic Tissues. *Int. J. Mol. Sci.* **2021**, *22*, 2622. https://doi.org/10.3390/ijms22052622.
35. Vassilev, L.T.; Vu, B.T.; Graves, B.; Carvajal, D.; Podlaski, F.; Filipovic, Z.; Kong, N.; Kammlott, U.; Lukacs, C.; Klein, C.; et al. In vivo activation of the p53 pathway by small-molecule antagonists of *MDM2*. *Science* **2004**, *303*, 844–848. https://doi.org/10.1126/science.1092472.

36. Wang, H.; Ma, X.; Ren, S.; Buolamwini, J.K.; Yan, C. A small-molecule inhibitor of *MDMX* activates p53 and induces apoptosis. *Mol. Cancer Ther.* **2011**, *10*, 69–79. https://doi.org/10.1158/1535-7163.MCT-10-0581.
37. Choong, M.L.; Yang, H.; Lee, M.A.; Lane, D.P. Specific activation of the p53 pathway by low dose actinomycin D: A new route to p53 based cyclotherapy. *Cell Cycle* **2009**, *8*, 2810–2818. https://doi.org/10.4161/cc.8.17.9503.
38. Alimirah, F.; Panchanathan, R.; Chen, J.; Zhang, X.; Ho, S.M.; Choubey, D. Expression of androgen receptor is negatively regulated by p53. *Neoplasia* **2007**, *9*, 1152–1159. https://doi.org/10.1593/neo.07769.
39. Azimian-Zavareh, V.; Hossein, G.; Janzamin, E. Effect of lithium chloride and antineoplastic drugs on survival and cell cycle of androgen-dependent prostate cancer LNCap cells. *Indian J. Pharmacol.* **2012**, *44*, 714–721. https://doi.org/10.4103/0253-7613.103265.
40. Löhr, K.; Möritz, C.; Contente, A.; Dobbelstein, M. p21/*CDKN1A* mediates negative regulation of transcription by p53. *J. Biol. Chem.* **2003**, *278*, 32507–32516. https://doi.org/10.1074/jbc.M212517200.
41. Benson, E.K.; Mungamuri, S.K.; Attie, O.; Kracikova, M.; Sachidanandam, R.; Manfredi, J.J.; Aaronson, S.A. p53-dependent gene repression through p21 is mediated by recruitment of *E2F4* repression complexes. *Oncogene* **2014**, *33*, 3959–3969. https://doi.org/10.1038/onc.2013.378.
42. Fischer, M. p21 governs p53's repressive side. *Cell Cycle* **2016**, *15*, 2852–2853. https://doi.org/10.1080/15384101.2016.1205393.
43. Fischer, M.; Quaas, M.; Steiner, L.; Engeland, K. The p53-p21-DREAM-CDE/CHR pathway regulates G2/M cell cycle genes. *Nucleic Acids Res.* **2016**, *44*, 164–174. https://doi.org/10.1093/nar/gkv927.
44. Peuget, S.; Selivanova, G. p53-Dependent Repression: DREAM or Reality? *Cancers* **2021**, *13*, 4850. https://doi.org/10.3390/cancers13194850.
45. Agrawal, R.; Sengupta, S. p53 regulates DREAM complex-mediated repression in a p21-independent manner. *EMBO J.* **2025**, *44*, 2279–2297. https://doi.org/10.1038/s44318-025-00402-7.
46. Innocente, S.A.; Lee, J.M. p53 is a NF-Y- and p21-independent, Sp1-dependent repressor of cyclin B1 transcription. *FEBS Lett.* **2005**, *579*, 1001–1007. https://doi.org/10.1016/j.febslet.2004.12.073.
47. Alinejad, V.; Hossein Somi, M.; Baradaran, B.; Akbarzadeh, P.; Atyabi, F.; Kazerooni, H.; Samadi Kafil, H.; Aghebati Maleki, L.; Siah Mansouri, H.; Yousefi, M. Co-delivery of IL17RB siRNA and doxorubicin by chitosan-based nanoparticles for enhanced anticancer efficacy in breast cancer cells. *Biomed. Pharmacother.* **2016**, *83*, 229–240. https://doi.org/10.1016/j.biopha.2016.06.037.
48. Ren, L.; Xu, Y.; Liu, C.; Wang, S.; Qin, G. IL-17RB enhances thyroid cancer cell invasion and metastasis via ERK1/2 pathway-mediated *MMP-9* expression. *Mol. Immunol.* **2017**, *90*, 126–135. https://doi.org/10.1016/j.molimm.2017.06.034.
49. Bie, Q.; Sun, C.; Gong, A.; Li, C.; Su, Z.; Zheng, D.; Ji, X.; Wu, Y.; Guo, Q.; Wang, S.; et al. Non-tumor tissue derived interleukin-17B activates IL-17RB/AKT/β-catenin pathway to enhance the stemness of gastric cancer. *Sci. Rep.* **2016**, *6*, 25447. https://doi.org/10.1038/srep25447.
50. Yang, Y.F.; Lee, Y.C.; Lo, S.; Chung, Y.N.; Hsieh, Y.C.; Chiu, W.C.; Yuan, S.F. A positive feedback loop of IL-17B-IL-17RB activates ERK/β-catenin to promote lung cancer metastasis. *Cancer Lett.* **2018**, *422*, 44–55. https://doi.org/10.1016/j.canlet.2018.02.037.
51. Ma, X.J.; Hilsenbeck, S.G.; Wang, W.; Ding, L.; Sgroi, D.C.; Bender, R.A.; Osborne, C.K.; Allred, D.C.; Erlander, M.G. The *HOXB13:IL17BR* expression index is a prognostic factor in early-stage breast cancer. *J. Clin. Oncol.* **2006**, *24*, 4611–4619. https://doi.org/10.1200/JCO.2006.06.6944.
52. Jerevall, P.L.; Ma, X.J.; Li, H.; Salunga, R.; Kesty, N.C.; Erlander, M.G.; Sgroi, D.C.; Holmlund, B.; Skoog, L.; Fornander, T.; et al. Prognostic utility of *HOXB13:IL17BR* and molecular grade index in early-stage breast cancer patients from the Stockholm trial. *Br. J. Cancer* **2011**, *104*, 1762–1769. https://doi.org/10.1038/bjc.2011.145.
53. Wang, H.; Liu, Y.; Yang, L.; Wang, Z.; Hou, Q.; Zhang, J.; Huang, W.; Ma, D. Differential roles of IL-17B and IL-17RB in colorectal cancer: Correlation with immune infiltration and prognosis. *Pathol. Res. Pr.* **2025**, *268*, 155847. https://doi.org/10.1016/j.prp.2025.155847.
54. Kim, K.H.; Nagappan, A.; Song, B.; Lim, S.; Moon, Y. Antibiotic-disrupted ribosome biogenesis facilitates tumor chemokine superinduction. *Biochem. Pharmacol.* **2022**, *206*, 115303. https://doi.org/10.1016/j.bcp.2022.115303.
55. Muniyan, S.; Pothuraju, R.; Seshacharyulu, P.; Batra, S.K. Macrophage inhibitory cytokine-1 in cancer: Beyond the cellular phenotype. *Cancer Lett.* **2022**, *536*, 215664. https://doi.org/10.1016/j.canlet.2022.215664.
56. Lu, L.; Johnson, C.H.; Khan, S.A.; Irwin, M.L. *GDF15* in the tumor microenvironment: A central mediator of cancer immunometabolism and therapeutic resistance. *Cytokine Growth Factor Rev.* **2026**, *88*, 47–57. https://doi.org/10.1016/j.cytogfr.2026.01.004.
57. Petersen, B.C.; Dolgachev, V.; Rasky, A.; Lukacs, N.W. IL-17E (IL-25) and IL-17RB promote respiratory syncytial virus-induced pulmonary disease. *J. Leukoc. Biol.* **2014**, *95*, 809–815. https://doi.org/10.1189/jlb.0913482.

58. Abdu, S.; Xia, J.; Yuan, H.; Tan, T.J.; Layhadi, J.A.; Shamji, M.H.; McKenzie, A.N.J.; Haloob, N.; Hopkins, C.; Woszczek, G.; et al. IL-25 Enhances B Cell Responses in Type 2 Inflammation Through IL-17RB Receptor. *Allergy* **2025**, *80*, 965–975. https://doi.org/10.1111/all.16472.
59. Fort, M.M.; Cheung, J.; Yen, D.; Li, J.; Zurawski, S.M.; Lo, S.; Menon, S.; Clifford, T.; Hunte, B.; Lesley, R.; et al. IL-25 induces IL-4, IL-5, and IL-13 and Th2-associated pathologies in vivo. *Immunity* **2001**, *15*, 985–995. https://doi.org/10.1016/s1074-7613(01)00243-6.
60. Wang, Y.H.; Angkasekwinai, P.; Lu, N.; Voo, K.S.; Arima, K.; Hanabuchi, S.; Hippe, A.; Corrigan, C.J.; Dong, C.; Homey, B.; et al. IL-25 augments type 2 immune responses by enhancing the expansion and functions of TSLP-DC-activated Th2 memory cells. *J. Exp. Med.* **2007**, *204*, 1837–1847. https://doi.org/10.1084/jem.20070406.
61. Deng, C.; Peng, N.; Tang, Y.; Yu, N.; Wang, C.; Cai, X.; Zhang, L.; Hu, D.; Ciccia, F.; Lu, L. Roles of IL-25 in Type 2 Inflammation and Autoimmune Pathogenesis. *Front. Immunol.* **2021**, *12*, 691559. https://doi.org/10.3389/fimmu.2021.691559.
62. Yuan, Q.; Peng, N.; Xiao, F.; Shi, X.; Zhu, B.; Rui, K.; Tian, J.; Lu, L. New insights into the function of Interleukin-25 in disease pathogenesis. *Biomark. Res.* **2023**, *11*, 36. https://doi.org/10.1186/s40364-023-00474-9.
63. Furuta, S.; Jeng, Y.M.; Zhou, L.; Huang, L.; Kuhn, I.; Bissell, M.J.; Lee, W.H. IL-25 causes apoptosis of IL-25R-expressing breast cancer cells without toxicity to nonmalignant cells. *Sci. Transl. Med.* **2011**, *3*, 78ra31. https://doi.org/10.1126/scitranslmed.3001374.

Disclaimer/Publisher's Note: The statements, opinions and data contained in all publications are solely those of the individual author(s) and contributor(s) and not of MDPI and/or the editor(s). MDPI and/or the editor(s) disclaim responsibility for any injury to people or property resulting from any ideas, methods, instructions or products referred to in the content.